Electrochemical characterization and regeneration of sulfur poisoned Pt catalysts in aqueous media

Chang-Hui Chen,[a] Adam Halford,[b] Marc Walker,[c] Colin Brennan,[d] Stanley C.S. Lai,[d] David J. Fermin,[e] Patrick R. Unwin[a,*] and Paramaconi Rodriguez[b, f*]

[a]*Department of Chemistry, University of Warwick, Gibbet Hill Rd, Coventry, CV4 7AL, U.K.*

[b]*School of Chemistry, University of Birmingham, Edgbaston, Birmingham, B15 2TT, U.K.*

[c]*Department of Physics, University of Warwick, Gibbet Hill Rd, Coventry, CV4 7AL, U.K.*

[d]*Syngenta, Jealott's Hill International Research Centre, Bracknell, Berkshire, RG42 6EY, U.K.*

[e]*School of Chemistry, University of Bristol, Cantock's Close, Bristol, BS8 1TS, U.K*

[f]*Birmingham Centre for Strategic Elements & Critical Materials, University of Birmingham, B15 2TT, U.K.*

*Corresponding authors

Patrick Unwin, P.R.Unwin@warwick.ac.uk

Paramaconi Rodriguez, P.B.Rodriguez@bham.ac.uk

ABSTRACT

Understanding the poisoning and recovery of precious metal catalysts is greatly relevant for the chemical industry dealing with the synthesis of organic compounds. For example, hydrogenation reactions typically use platinum catalysts and sulfuric acid media, leading to poisoning by sulfur-containing species. In this work, we have applied electrochemical methods to understand the status and recovery of Pt catalysts by studying the electro-oxidation of a family of sulfur-containing species adsorbed at several types of Pt electrodes: (i) polycrystalline Pt foil; (ii) Pt single-crystal electrodes; and (iii) Pt nanoparticles supported on Vulcan carbon. The results obtained from polycrystalline Pt electrodes and Pt nanoparticles supported on Vulcan carbon demonstrate that all sulfur-containing species with different oxidation states (2-, 3+ and 4+) lead to the poisoning of Pt active sites. X-ray photoelectron spectroscopy (XPS) analysis was employed to elucidate the chemical state of sulfur species during the recovery process. The degree of poisoning decreased with increased sulfur oxidation state, while the rate of regeneration of the Pt surfaces generally increases with the oxidation state of the sulfur species. Finally, the use of Pt single-crystal electrodes reveals the surface-structure sensitivity of the oxidation of the sulfur species. This information could be useful in designing catalysts that are less susceptible to poisoning and/or more easily regenerated. These studies demonstrate voltammetry to be a powerful method for assessing the status of platinum surfaces and for recovering catalyst activity, such that electrochemical methods could find applications as sensors in catalysis and for catalyst recovery in-situ.

KEYWORDS

Pt catalysts, sulfur poison, cyclic voltammetry, XPS, single-crystal electrode

HIGHLIGHTS

- The poisoning of Pt catalysts from sulfur compounds with sulfur in different oxidation states of, 2-, 3+ and 4+ was studied.
- Poisoned Pt catalysts can be renewed by consecutive potential cycling with an upper potential limit of 1.25 V versus RHE.
- XPS analysis has demonstrated the conversion of sulfur to sulfate during the voltammetric regeneration.
- Pt single-crystal electrodes revealed surface-structure sensitivity of the electro-oxidation of the adsorbed sulfur species.

GRAPHIC ABSTRACT

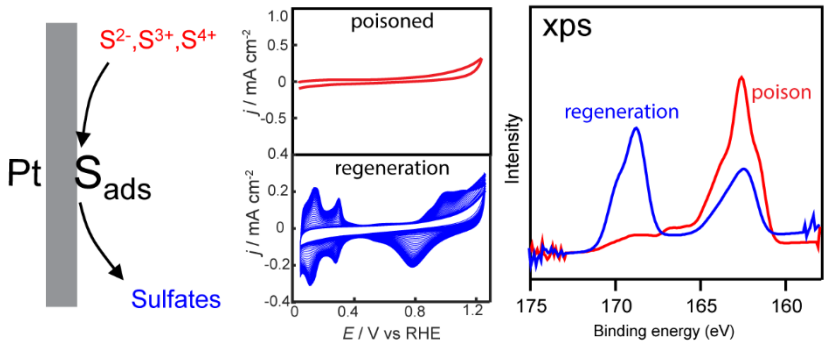

INTRODUCTION

The deactivation of metal catalysts due to the adsorption of sulfur and sulfur-containing compounds is a great concern in many chemical industrial applications, e.g. the widely employed hydrogenation/dehydrogenation, hydrocracking, and the oxidation of hydrocarbons processes [1-5]. The deactivation leads to the replacement and disposal of precious metal catalysts (platinum group) [6] on a regular basis [1, 3], with tremendous economic impact on the cost of the industrial process.

Elemental sulfur and sulfur-containing species are among the sources of such deactivation processes [1, 3, 7]. These species strongly adsorb on many metals and change their catalytic properties by blocking surface active sites [8], modifying the electronic structure of the Pt surface [8, 9], or changing the adsorption behaviour of reactants [10, 11]. The source of elemental sulfur and sulfur-containing species is diverse, e.g. the carbon support [12, 13], the reactant feedstock [14], and the solvent [3]. As such, there is a need to understand the poisoning process of a range of sulfur-containing species at a fundamental level and determine efficient ways to recover the activity of catalysts.

Previous studies have implemented electrochemical tools to remove adsorbed sulfur species from Pt via electro-oxidation [15-19]. So far, most studies in the literature have dealt with poisoning from sulfide (Na_2S or H_2S) [15-17, 20-23] and SO_2 [13, 24-27]. The extensive and repetitive use of cyclic voltammetry over a wide potential range has been shown to lead to essentially complete removal of sulfur species, due to the formation of (bi)sulfates, which are soluble in water and do not bind irreversibly at Pt surfaces [28-30].

The overall oxidation reaction of Na_2S (or H_2S) to SO_4^{2-} occurs by a transfer of $8H^+/6e^-$ [15],

$$\mathrm{Pt-S_{ads}+4H_2O \rightleftharpoons SO_4^{2-}+8H^+ + 6e^- + Pt} \quad (1)$$

while the overall oxidation reaction of SO_2 to SO_4^{2-} follows a $4H^+/2e^-$ transfer reaction [15]:

$$\mathrm{Pt-SO_{2,ads}+2H_2O \rightleftharpoons SO_4^{2-}+4H^+ + 2e^- + Pt} \quad (2)$$

These are multistep complex processes, and the reaction pathway depends on reaction temperature [31, 32], sulfur coverage (θ_S) [22], the presence of oxygen [19, 28] and applied oxidation potential limit [33, 34]. Ramaker *et al.* reported the potential-dependent oxidation of sulfur species on Pt and Pt_3Co supported nanoparticles [30]. Using X-ray absorption spectroscopy, the authors suggested that at high potentials (E > 0.6 V vs reversible hydrogen electrode (RHE)), the adsorption of O or OH species was essential for the oxidation of sulfur species to (bi)sulfates. The oxidation was followed by the desorption of (bi)sulfate species at lower potential. As a result, consecutive potential cycling produced free Pt sites in each cycle, assisting the removal of sulfur species. Surface spectroscopy analysis, such as Auger electron spectroscopy [17, 28], in situ X-ray photoelectron spectroscopy (XPS) [13, 29], surface enhanced Raman spectroscopy (SERS) [21, 22], and Fourier Transform Infrared (FTIR) spectroscopy [35-37] have also been implemented in order to provide further evidence of the chemical state of sulfur during electrochemical-oxidation processes.

The poison effect of a broad variety of sulfur species, e.g. S^{2-}, S^0, S-O, SO_2/SO_3^{2-}, is not yet well known. Understanding the potential and surface-structure dependence of the oxidation of different sulfur species at platinum electrodes would give new insights into the general electro-oxidation mechanisms, and allow identification of new ways to avoid poisoning and for electrochemical recovery of poisoned Pt catalysts.

In this work we report on the irreversible adsorption of sulfur-containing species and the subsequent electrochemical regeneration of polycrystalline Pt, Pt single-crystal and Pt

nanoparticles (PtNPs) supported on carbon electrodes. Studying this range of Pt-based materials is important because the structure of Pt surfaces also has an impact on the adsorption [38] and regeneration of Pt surfaces [12, 13, 28, 39]. This study investigates a wide range of sulfur-containing species: Na_2S, $Na_2S_2O_4$, $Na_2S_2O_5$, Na_2SO_3 and SO_2. The regeneration of the active sites of the Pt electrodes was achieved by potential cycling in sulfuric acid solution and the chemical nature of adsorbed species was determined by *ex situ* XPS.

EXPERIMENTAL

Chemicals and Materials. Sulfuric acid (96% Suprapur®, Merck), $Na_2S{\cdot}9H_2O$ (≥ 99.99 %, Sigma-Aldrich), $Na_2S_2O_4$ (~85 %, Sigma-Aldrich), $Na_2S_2O_5$ (≥ 93 %, Fisher Chemicals), and Na_2SO_3 (ACS reagent, anhydrous, ≥ 98.0 %, Sigma-Aldrich) were used as received. A solution containing 0.1 M SO_2 was prepared by adding the required amount of Na_2SO_3 in 10 mL acid solution (H_2SO_4). All aqueous solutions were freshly prepared before each experiment from ultra-pure water (Millipore Corp., 18.2 MΩ cm resistivity at 25 °C).

***Preparation of electrodes*.** Three types of working electrodes were used in this work: polycrystalline Pt foils, PtNPs on Vulcan carbon modified glassy carbon electrodes (PtNP/C), and Pt single-crystal electrodes.

Pt foil electrode**.** Pt foil (> 99.95 %, 0.125 mm thickness; Advent Research Materials) electrodes were made by hanging a piece of foil on a thin Pt wire (diameter 250 μm), with the wire inserted into a glass tube. The surface area was controlled to an approximate extent, by only immersing the foil in the electrolyte solution. The current densities reported in this worked were normalized to the electrochemical surface area (ECSA) of each electrode, which was determined from a fully regenerated (clean) CV. In each ease, the ECSA was calculated by integrating H_{UPD} region of a clean Pt CV and using the theoretical value of 210 μC cm^{-2} for the formation of a hydrogen monolayer [40].

PtNP/C. Commercial 20 % wt Pt/C Vulcan (ETEK) was deposited on a substrate electrode, following a method as described elsewhere [41]. The catalyst ink was diluted with water and had a final concentration of (7.00 ± 0.01) $\times 10^{-2}$ g L^{-1} of Pt [42]. A rotating disk electrode (RDE) with a glassy carbon electrode inset (RDE, 5 mm diameter, Pine Instrument) was hand-polished on a cloth impregnated with an aqueous suspension of 0.05 μm alumina particles, followed by thorough rinsing with ultra-pure water. The freshly cleaned RDE was then mounted onto the inverted shaft of an electrode rotator and a droplet of 35 μL catalyst ink was drop-casted onto the substrate. To obtain a homogenous film, the RDE was rotated at 700 rpm for 1 h until the film was completely dry. An optical microscopic image of a typical dried electrode is provided in Supporting Information (Section S1). It can be seen that a uniform deposit of catalyst was achieved. The current density for each PtNP/C electrode was also normalized to its ECSA, following the same method for Pt foil electrodes.

Single-crystal Pt electrodes. Single-crystal measurements were performed on bead-type Pt single-crystal electrodes with surface orientations of (100), (111) and (221) (icryst, Jülich, Germany). Prior to each experiment, the electrodes were flame annealed by a butane torch for 1 min and cooled down in a H_2/Ar atmosphere (ca. 1:3 in flow rate) for 1 min. Then, they were protected with deaerated ultra-pure water (with Ar), and transferred to the electrochemical cell in equilibrium with an Ar atmosphere.

Electrode modification with sulfur compounds. Treatment of different Pt electrodes was carried out at open circuit potential (OCP) conditions in aerated solutions. In each case, the Pt electrode (foil, PtNP/C, or single-crystal) was immersed in 0.1 M aqueous solution containing a sulfur compound of interest. The open circuit potential was recorded as a function of time for the Pt(111) and Pt(100) single crystal electrodes upon immersion in the solutions. Single-crystal electrodes were immersed for 1 minute, while the Pt foil and PtNP/C electrodes (which

had a large specific surface area) were immersed for 5 minutes. The resulting sulfur-modified Pt electrodes were rinsed copiously with ultra-pure water to remove any excess sulfur-compound. Finally, they were transferred into electrochemical cells containing clean H_2SO_4 electrolyte for electrochemical measurements.

Electrochemical measurements. Electrochemical measurements on Pt foils and PtNP/C electrodes were carried out in a three-electrode configuration, using either a CHI potentiostat (CHI1105a, CH Instruments, USA) or an Autolab PGSTAT12 potentiostat. Pt (99.99 %, MaTeck/Alfa Aesar) foils were used as counter electrodes. The reference electrode was a palladium wire saturated with absorbed hydrogen (Pd-H_2), prepared by evolving hydrogen on the palladium (Pd) wire. All potentials reported herein are against the reversible hydrogen electrode (E^0(Pd-H_2) = 50 mV vs RHE) [43]. Unless otherwise indicated, all aqueous solutions were deaerated with nitrogen prior to electrochemical studies.

Experiments on single-crystal working electrodes were performed in a 2-compartment cell where the Pd-H_2 reference electrode was connected via a Luggin capillary. All glassware used for single-crystal measurements was cleaned by immersing in an acidic solution of potassium permanganate overnight, followed by rinsing with ultra-pure water and pre-mixed cleaning fluid (1 mL H_2SO_4 and 3 mL H_2O_2 in 1 L water), then repeated heating and rinsing with ultra-pure water.

X-ray photoelectron spectroscopy (XPS) measurements. XPS measurements were made at room temperature (*ca.* 20 °C) in the main analysis chamber of an Omicron Multiprobe ultra-high vacuum instrument (base pressure 2×10^{-10} mbar), with the sample being illuminated using an XM1000 monochromatic Al k_α X-ray source (Omicron Nanotechnology) at a take-off angle of 90° with respect to the sample surface. The photoelectrons were detected using a Sphera electron analyzer (Omicron Nanotechnology), with the core level spectrum recorded

using a pass energy of 10 eV (resolution approx. 0.47 eV). The Pt foils investigated in this study were mounted on Omicron sample plates using electrically-conductive carbon tape and loaded into the fast-entry chamber. Once a pressure of less than 1 x 10^{-7} mbar had been achieved (approx. 1 hour), the samples were transferred to a 12-stage storage carousel, located between the preparation and main analysis chambers, for storage at a pressure of less than 2×10^{-10} mbar. The data were analyzed using the CasaXPS package, using Shirley backgrounds, mixed Gaussian-Lorentzian (Voigt) line shapes and asymmetry parameters where appropriate. All binding energies were calibrated using the Fermi edge of a polycrystalline Ag sample, measured immediately prior to commencing the measurements. Compositional accuracy was ensured by calibrating the transmission function of the spectrometer using a variety of clean metal foils.

In order to minimize contamination of the samples due to exposure to air, all samples were prepared immediately before the XPS analysis, rinsed with ultra-pure water and transferred to the XPS chamber directly after the electrochemical treatment (within 1 minute).

RESULTS AND DISCUSSION

Electrochemical characterization of clean and sulfur-poisoned polycrystalline Pt electrode

Polycrystalline Pt foil electrodes were investigated first. In this work, five sulfur compounds, Na_2S, $Na_2S_2O_4$, $Na_2S_2O_5$, Na_2SO_3 and SO_2, were evaluated.

Fig. 1 shows cyclic voltammograms (CVs) of sulfur-compound treated Pt foil electrodes in a N_2-saturated 50 mM H_2SO_4 solution. Blank CVs recorded at clean foils are also provided, for ease of comparison. Two characteristic potential regions can be distinguished in the blank CV: (i) the potential region between 0.0 – 0.45 V associated to the hydrogen adsorption/desorption (H_{ads}/H_{des}) [44, 45] and (ii) the potential region between 0.70 – 1.25 V

associated to the formation and reduction of surface oxides [44, 45]. Fig. 1a highlights the significant difference in the voltammetric profile between a clean Pt surface and one treated with Na_2S. Clearly, after Na_2S treatment (experimental section), the features associated to H_{ads}/H_{des} and surface oxide formation/reduction of a clean Pt polycrystalline surface were completely suppressed. In contrast, for Pt foils modified by $Na_2S_2O_4$, $Na_2S_2O_5$, Na_2SO_3 and SO_2 (Fig. 1b-1e), the H_{ads}/H_{des} features are partly retained, indicating the Pt surfaces were only partially blocked by treatment with these sulfur compounds on the same time scale of 5 minutes. This might suggest the adsorption of these species requires a specific atomic assembly [46].

For surface modified Pt electrodes, at potentials higher than 0.9 V, sharp oxidation features were observed in all cases (Fig. 1, solid line). This can be assigned to the electro-oxidation of adsorbed sulfur-moieties, S_{ads}, formed at the Pt surfaces. The fractional coverage of these sulfur species (θ_S), can be determined using [15, 16]:

$$\theta_S = \frac{Q_H^0 - Q_H^S}{Q_H^0} \quad (3)$$

where Q_H^0 and Q_H^S are the hydrogen charge density of a clean and poisoned Pt surface, respectively. In this paper, Q_H^0 of 210 μC cm^{-2} is used. Q_H^S was calculated by dividing the hydrogen desorption charge (in the first anodic scan) by the corresponding ECSA obtained from a clean Pt surface (experimental section). θ_S is the fraction of covered sites on Pt. $\theta_S = 0$ corresponds to a clean surface and $\theta_S = 1$ corresponds to a fully blocked surface. The values of charge Q_H^S, and the sulfur coverage θ_S calculated for each species are listed in Table 1.

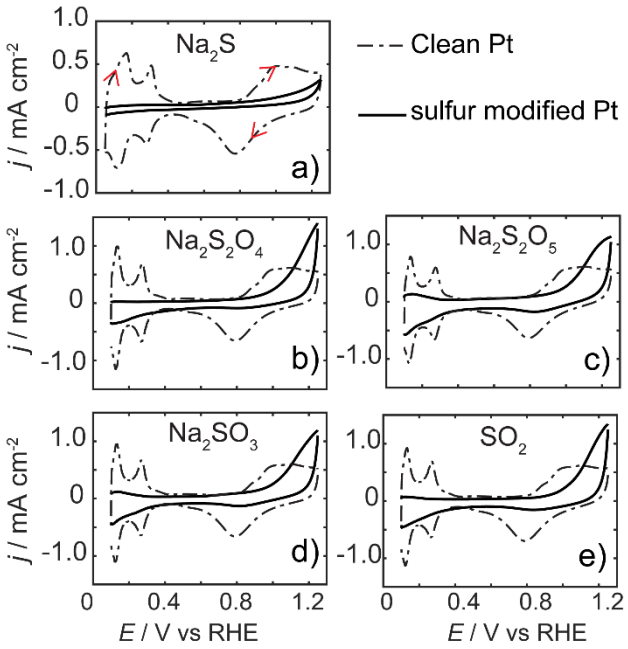

Figure 1. Voltammetric profiles of polycrystalline Pt foil electrodes obtained before (dash-dotted line) and after (solid line) immersing in 0.1 M (a) Na_2S, (b) $Na_2S_2O_4$, (c) $Na_2S_2O_5$ (d) Na_2SO_3 and (e) SO_2 solutions for 5 minutes. All CVs were recorded in 50 mM H_2SO_4 at a scan rate υ = 500 mV s^{-1}. Scan directions are shown in Fig.1a by red arrows.

Table 1. Values of the Q_H^S and θ_S determined from CVs in Fig. 1.

	Na_2S	$Na_2S_2O_4$	$Na_2S_2O_5$	Na_2SO_3	SO_2
Q_H^S (μC cm^{-2})	0	2.7	23.8	19.2	8.7
θ_S	100 %	99 %	89 %	91 %	96 %

Q_H^S: Hydrogen desorption charge at sulfur compound modified Pt.
θ_S: sulfur species coverage (as determined by equation (3)).

Electrochemical regeneration of sulfur-modified polycrystalline Pt electrodes

The regeneration of sulfur-modified Pt electrodes was conducted by consecutive potential cycling, with an upper potential limit of 1.25 V. Each cycle resulted in the partial oxidation/desorption of sulfur-containing adsorbates from the Pt surface. Regeneration CVs for each of the sulfur-modified electrodes are shown in Fig. 2a-2e.

As can be seen, in all figures, upon consecutive cycling up to 1.25 V, the features associated to the H_{ads}/H_{des} on the Pt electrode gradually reappear with increasing cycle number. Fig. 2a shows CVs for the regeneration of a Pt electrode modified in a Na_2S solution. Besides the increase of H_{ads}/H_{des} current, there is an also an increase of the oxidation current at potentials higher than 0.8 V. This current is associated with the oxidation of the adsorbed sulfur species but is also due to the formation of surface oxides e.g. OH_{ads} and O_{ads} [44]. Simultaneously with the increase of the anodic currents, the voltammetric profile also displays an increase of current associated to the reduction of platinum oxides. It is important to notice that after 15 cycles, the current in the potential region between 0.78 and 1.13 V continues to increase with cycle number, while the current at potentials higher than 1.13 V starts to decrease. Such behaviour results in the appearance of an isopotential point (E_{iso}) at 1.13 V. The E_{iso} herein is consistent with those reported in the literature [17]. We propose that the E_{iso} corresponds to a change in the dominant reaction in the potential window between 0.8 and 1.25 V. During the first 15 scans, under a high S_{ads} coverage (θ_S), the oxidation of S_{ads} at E > 1.13 V is the dominant reaction, while the oxidation of Pt surface has minor contribution. After 15 cycles, θ_S decreases and more Pt atoms are available for the formation of surface oxides (0.78 –1.13 V). This results in the decrease of the oxidation current at potentials higher than 1.13 V. After 50 cycles, the poisoned Pt electrode was only partially recovered, achieving a hydrogen charge of 82.0 μC cm^{-2}, which is only 39 % of a clean electrode (210 μC cm^{-2}).

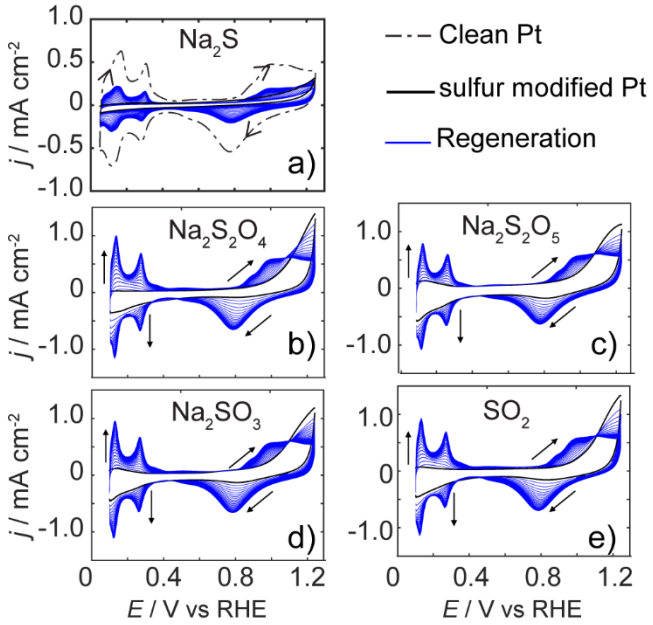

Figure 2. Series of cyclic voltammograms for Pt electrodes after surface modification in (a) Na_2S, (b) $Na_2S_2O_4$, (c) $Na_2S_2O_5$ (d) Na_2SO_3 and (e) SO_2 solution as described in the experimental methods. The first CVs of recorded at sulfur-modified Pt electrode are marked as bold black. The blue lines (increasing current) correspond to the consecutive cycles during regeneration. In Fig. 2a, 50 cycles were recorded while in Fig. 2b-2e only 25 cycles were required for essentially full recovery of the surface. Fig. 2a also displays the blank voltammogram of the Pt electrode without surface modification, as indicated with a dash-dotted line. All CVs were recorded in 50 mM H_2SO_4. Scan rate: υ = 500 mV s^{-1}.

In contrast to the surface modification with Na_2S, results for a Pt electrode immersed in $Na_2S_2O_4$ (b), $Na_2S_2O_5$ (c), Na_2SO_3 (d), and SO_2 (e) showed lower degrees of sulfur coverage, θ_S, and quicker recovery. After 25 cycles, the CV profiles at regenerated Pt electrodes were essentially identical to the clean ones. A similar isopotential point was also observed during regeneration for these species at potentials close to 1.10 V, suggesting the oxidation processes (and thus the adsorbed species) are similar in all cases.

In order to provide a quantitative analysis of the oxidation process of the adsorbed species, the charge densities associated to the hydrogen adsorption, in the cathodic sweeps were plotted as a function of voltammetric cycle number. Notably, in Fig. 3, the first data point is after the first anodic stripping. Combining results in Fig. 2 and 3, it is clear that the change of hydrogen charge density strongly depends on the nature of the sulfur compound. For Na_2S treated surfaces, the recovery was slow during the first 15 cycles. Afterwards, the charge grows rapidly and slows down again after 30 cycles. For all other species, the hydrogen charge increases rapidly in the first 10 cycles and reaches a plateau after 23 cycles.

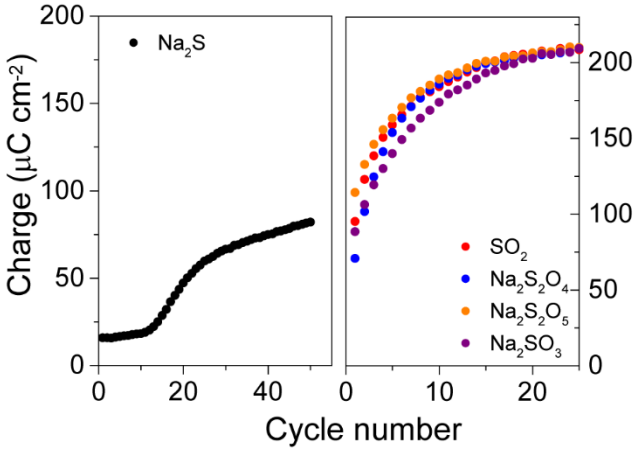

Figure 3. Relation between the hydrogen charge density and the corresponding number of voltammetric cycles. All charge values were obtained from the integration of the cathodic scan in the potential region of 0.05 – 0.45 V (after double layer subtraction) from Fig. 2. The key represents the species used to modify the Pt surface.

The slow regeneration of Pt electrodes after exposure to Na_2S has been observed in previous studies [11, 28].The slow recovery at high θ_S means that few OH adsorption sites are available on the surface during the first few cycles, but as more free Pt sites are created, which increases the number of OH species adsorbed, there is a sharp increase in the oxidation rate of S^{2-} species on the surface.

XPS investigation of the regeneration of sulfur-modified Pt electrodes

XPS analysis was performed at different stages of the recovery process, to determine the nature of the intermediates species during the oxidation reaction. The three stages are: i) as-prepared (directly after poisoning); ii) after a few voltammetric cycles (partially regenerated) iii) after more extensive cycling.

Fig. 4 compares the XPS spectra from the S 2*p* energy level for polycrystalline platinum modified in a Na_2S solution. In the spectrum of the as-prepared electrode (Fig. 4a), a broad feature at 162.5 eV is observed. Deconvolution of the spectrum reveals three S $2p_{3/2}$ components at binding energies of 161.52 eV, 162.53 eV and 164.63 eV, corresponding to sulfides (S^{2-}), S-S/S-metal, and S^0, respectively (note that the corresponding S $2p_{1/2}$ components are located at + 1.18 eV from the S $2p_{3/2}$ component). The XPS spectrum reveals the complexity of sulfur adsorption from a Na_2S solution, with both neutral and negatively charged sulfur found on the Pt surface. This result is consistent with the previous studies by Tong *et al.* [22], who reached similar conclusion using surface-enhanced Raman spectroscopy and by Wieckowski's group from high-resolution Auger electron spectroscopy (AES) and core-level electron-energy loss spectroscopy (CEELS) [28]. Full survey spectra covering binding energy range of 0 – 1400 eV and the element analysis are shown in the Supporting Information (Sections S2 – S4) and demonstrate the changes of the relative concentrations of elements during potential cycling.

The spectrum in Fig. 4b corresponds to a partially regenerated electrode, after 15 voltammetric cycles up to an anodic limit of 1.25 V. For this sample (II), the band intensity at 162.5 eV has decreased in comparison with sample I. Meanwhile, a new band at ~168.9 eV appears, which can be assigned to sulfates/sulfites. Due to their close energy levels, XPS is not capable of differentiating between the two species [47]. Nonetheless the change of the XPS

spectrum in Fig. 4b, relative to that in Fig. 4a, clearly indicates that adsorbed S^{2-} was oxidized to sulfates/sulfites through voltammetric cycling [29].

After 50 cycles, the XPS spectrum of sample III (Fig. 4c) shows a significant decrease of the signal at 162.5 eV and the band at ~168.9 eV has disappeared, indicating the removal of sulfate/sulfite groups. The integrated values of the bands associated to the sulfur species at the three different regeneration stages are summarized in Table 2.

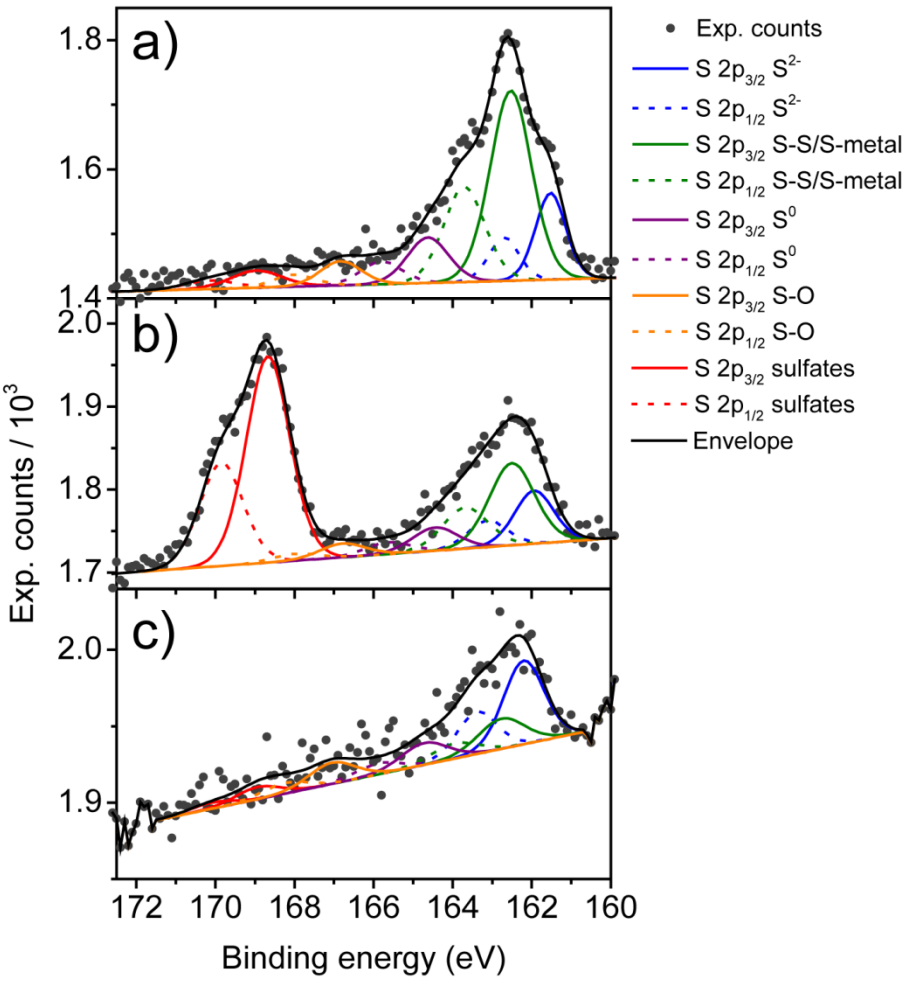

Figure 4. S 2*p* XPS spectra recorded on Pt foils with: a) Na_2S treatment; b) after partial regeneration (15 voltammetric cycles between 0 – 1.25 V at 500 mV S^{-1}); c) after 50 equivalent voltammetric cycles. The circles mark the experimental results, and the black line is the global fit

of the data. The S 2$p_{3/2}$ and S 2$p_{1/2}$ peaks are marked with solid and dashed color line, respectively. The bond energies of S 2$p_{3/2}$ peaks are summarized in Supporting Information (Table S2).

Table 2. Summary of XPS results of sulfur modified- and cleaned- Pt electrodes.

Na_2S						
	S_{ads}/S_{total} (%)					
Sample	S^{2-}	S-S/S-metal	S^0	S-O	sulfates or sulfites	S_{total}/Pt (%)
I (modified)	18.35	55.25	13.16	7.06	6.18	27.88
II (partly cleaned)	12.55	22.62	6.41	3.78	54.64	25.83
III (cleaned)	45.98	19.18	13.89	13.52	7.42	4.04

Na_2SO_3				
	S_{ads}/S_{total} (%)			
Sample	S-S/S-metal	S^0	sulfates or sulfites	S_{total}/Pt (%)
I′ (modified)	17.45	4.00	78.55	19.36
II′ (partly cleaned)	10.11	0	89.89	14.87
III′ (cleaned)	0	0	100.00	17.25

For Pt foil modified by Na_2S, after 15 cycles, the ratio of S_{total}/Pt remains almost unaltered (see Table 2). However, the percentage of sulfate(sulfite) has increased from 6.18 % to 54.64 %, confirming the oxidation of S_{ads} to these species. After 50 cycles, the ratio of S_{total}/Pt decreased further to 4.04 % and the amount of sulfate/sulfite has also decreased, suggesting the desorption of sulfur-containing species that are soluble in water. The increase of S^{2-}, by proportion, on sample III is not associated to an increase of the S^{2-} adsorbed, but to a decrease of the total amount of sulfur species adsorbed (S_{total}).

Fig. 5 compares the S 2*p* spectra of the as-prepared polycrystalline Pt treated with Na_2SO_3 (a), the surfaces after 5 (b), and 25 (c) voltammetric cycles. In contrast to the results in Fig. 4, the spectrum for the as-prepared Pt electrode shows a more intensive contribution at 168.9 eV, attributed to the sulfate and sulfite species present on the surface. In Fig. 5a, the deconvolution of the band at 163.0 eV also shows trace amount of S^0 and S-S. As the

regeneration process takes place, the band intensity at 163.0 eV has decreased substantially after five cycles (Fig. 5b) and disappeared after 25 cycles. At a regenerated Pt surface (Fig. 5c), only sulfates (SO_3^{2-} or SO_4^{2-}) can be found on the surface (see Table 2).

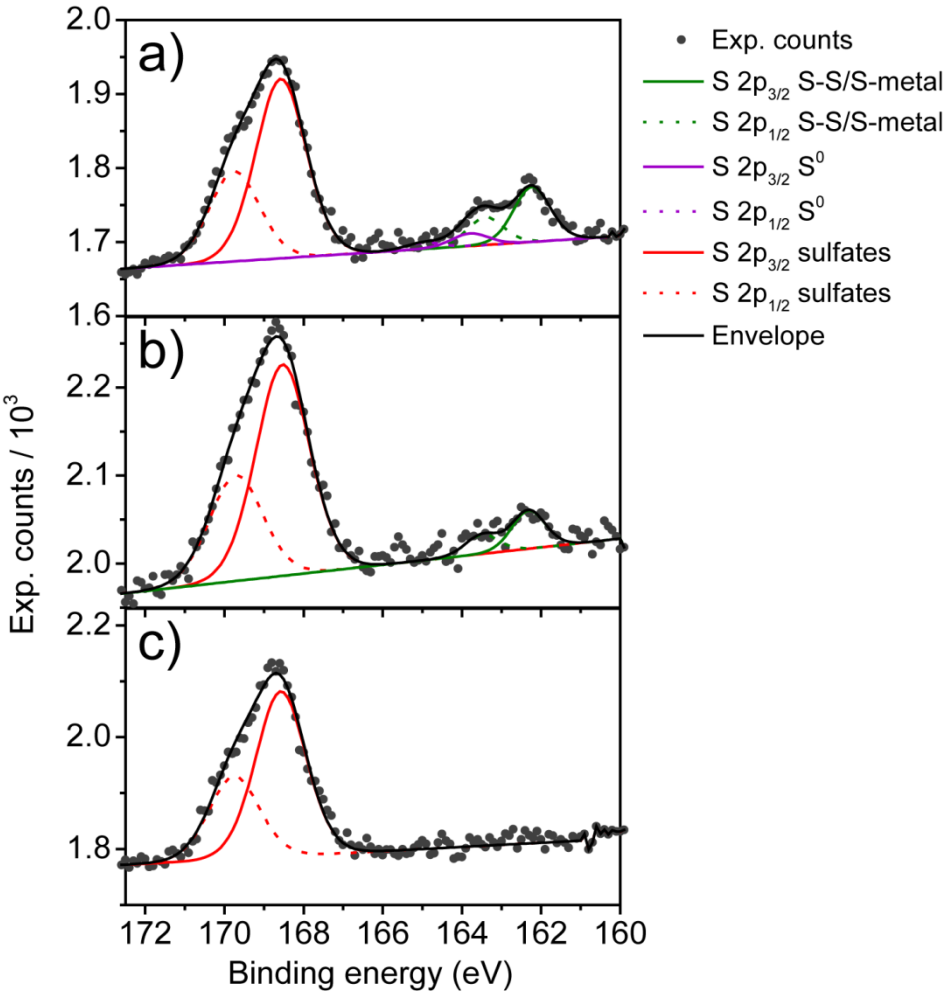

Figure 5. S 2*p* spectra recorded on Pt foils with: a) Na_2SO_3 treatment; b) after partial regeneration (5 voltammetric cycles between 0 – 1.25 V at 500 mV S^{-1}); c) after 25 equivalent voltammetric cycles. The circles mark the experimental results, and the black line is the global fit of the data. The S $2p_{3/2}$ and S $2p_{1/2}$ peaks are marked with solid and dashed color line, respectively. The bond energies of S $2p_{3/2}$ peaks are shown in Supporting Information (Table S2).

Electrochemical characterization of sulfur-modified Pt single-crystal electrodes

In order to further elucidate the nature of the adsorbed species, the voltammetric regeneration experiments were performed on three different types of Pt single-crystals, with orientation (100), (111) and (221) [Pt(3) (111) × (110)]. The purpose of these experiments was to provide insights into the surface-structure sensitivity of the oxidation reaction of adsorbed sulfur species. Measurements focused on Na_2S-treated surfaces, as the studies on polycrystalline Pt, reported above, revealed this as the most difficult species to remove. For comparative purpose, further measurements were made on Na_2SO_3 treated-surfaces (see below).

The open circuit potential upon immersion of the electrode in the Na_2S and Na_2SO_3 solution was measured as a function of time in independent experiments (Figure S5). The solutions were air-saturated in order to reproduce the conditions used during the modification/oxidation experiments. These measurements allowed us to study the dynamics of the charge transfer process during the poisoning of the electrode surface. It was observed that upon immersion the OCP shifted rapidly (< 20 s) to less positive potentials for both single-crystals electrodes in the Na_2S and Na_2SO_3 solutions. Similar behaviour has been observed for the adsorption of thiols on gold electrodes [48]. After the rapid change, the OCP reached a plateau during the rest of the measurement (+ 40 s). This suggests that on the small surface area of the single-crystal electrodes, the surface poisoning takes place within the first 30 s. The observed shift of the OCP is attributed to the accumulation of negative charge on the electrode through the donation of electron density from sulfur species to the platinum electrode. The slope of the change of the OCP with time indicates that the rate of adsorption is almost independent of the surface structure for the Na_2S, but is faster on the Pt(111) for the Na_2SO_3. The magnitude of the shift of the OCP, for both Pt(111) and Pt(100) is larger for the modification of the electrode in Na_2S in comparison with the modification with Na_2SO_3.

Although, the relative change of the magnitude of the OCP could be associated to the maximum coverage of the species in both crystallographic structures, other factors such as the surface dipole of the adsorbed species, rearrangement of the water layer, ionic distribution across the double-layer region may affect the change in the OCP magnitude. In addition, the effect of different amounts of dissolved oxygen in the solution for each experiment cannot be ruled out since at these potentials Pt electrodes are active towards the oxygen reduction reactions, which would affect the OCP measurement.

Fig. 6 shows the first two consecutive scans of each Pt single-crystal electrode modified in a Na_2S solution. The blank CVs (dash-dotted lines) in the absence of sulfur adsorbed species have also been included for sake of comparison. Detailed descriptions of the blank CVs can be found in Supporting Information (Section S6).

Blank CVs of Pt(100), Pt(111) and Pt(110) surfaces showed typical features associated to H_{des} (anodic sweep) in sulfuric acid solution in the potential range of 0.0 – 0.6 V [49, 50]. At more positive potentials, the surface oxidation/reduction of the Pt single-crystal takes place. As a result of the high potential limits, the surface structure is disturbed and the fingerprints associated to H_{ads} on each surface structure are affected [51]. This can be seen from the cathodic sweep of the blank CVs (particularly on Pt(100) and Pt(111)), where new features associated to H_{ads} on surface defects are noticeable (Supporting Information, Fig. S4). Similar to the results obtained at Pt foil electrodes, after immersing in Na_2S solutions, there was complete suppression of the H_{des} signature in the first anodic sweep for all the three single-crystal electrodes. At higher potentials, the CV features clearly show a surface sensitivity of the oxidation reaction.

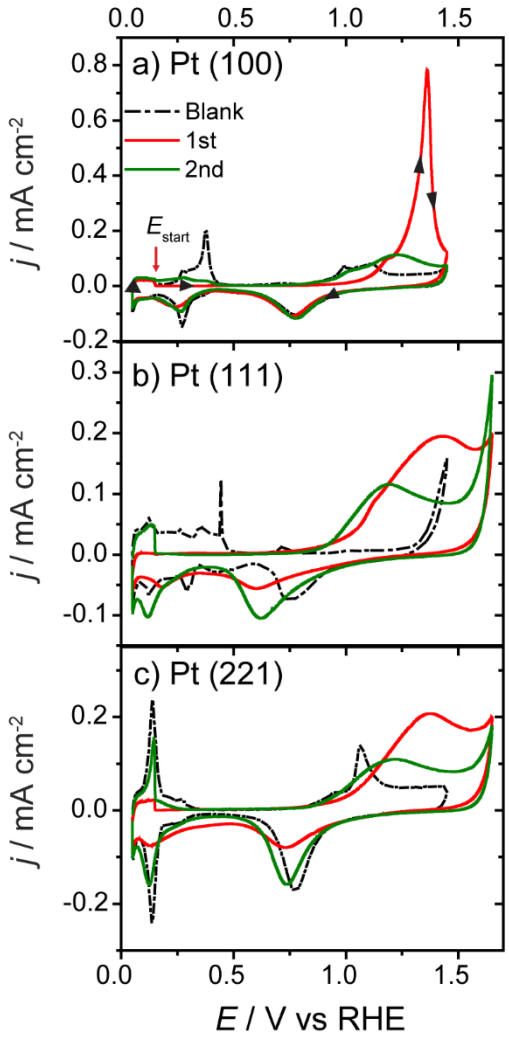

Figure 6. Voltammetric profiles in 0.5 M H_2SO_4 of Na_2S treated Pt(100), Pt(111), and Pt(221) electrodes. The dash-dotted line corresponds to the unmodified Pt single-crystal electrodes, while the red and green curves illustrates the first and second scan of a modified electrode. Arrows in Fig. 6a indicate the starting potential and scan directions. Scan rate, υ = 50 mV s^{-1}.

On Pt(100), in the first anodic sweep, the oxidation of S_{ads} starts at ~0.93 V, followed by a pre-wave at ~1.15 V and a sharp peak centered at ~1.36 V. It is important to notice that the onset of S_{ads} oxidation starts at a more positive potential than the oxide formation on bare Pt(100) (~0.8 V). Upon the first cathodic scan, the charge associated with oxide reduction, between 0.65 and 0.95 V on a modified Pt surface, is identical to the blank CV, suggesting a

(near) complete removal of the S_{ads}. However, the features at low potentials (0.0 – 0.4 V) are more complex. First, although there is a clear sign of S_{ads} removal during the anodic scan, the H_{ads} charge for the first CV is still significantly lower than for the blank CV. Furthermore, the charge for H_{ads} in the first cathodic and H_{des} in the second anodic sweep are different. Both features indicate that an adsorption of solution species other than protons has taken place in the low potential region, which blocks Pt active sites. These adsorbed species are presumably reaction intermediates or products from S_{ads} oxidation.

In the second scan, the onset of S_{ads} oxidation appears at a lower potential and coincides with the onset of the oxidation of a bare electrode (~0.80 V vs RHE). Interestingly, besides the large charge contribution observed in the second oxidation cycle, the H_{ads} current in the second cycle does not change significantly with respect to the first one. This suggests that the products from S_{ads} oxidation remain strongly adsorbed on the Pt(100) surface, which are difficult to oxidize further upon cycling between 0.0 – 1.5 V vs RHE. This is also evidenced by the stability of the CVs and lack of further recovery of the surface even after 3 oxidation cycles (Supporting Information, Fig. S6).

In Fig. 6b and 6c, the voltammetric profiles for S_{ads} oxidation on the Pt (111) and Pt(221) electrode are significantly different to Pt(100). At Pt(111) and Pt(221), the onset for S_{ads} oxidation appears at ~0.9 V, and the CVs show a broad peak centred at 1.43 V. Due to the shift of the oxidation peak towards more positive potentials, the upper potential window was increased up to 1.65 V. In contrast to our results, previous studies on the oxidation of sulfur on Pt(111) showed a sharp peak centred at 1.0 V vs RHE in H_2SO_4 solution [28, 32]. This is because the S_{ads} adlayer is sensitive to the adsorption potential, Na_2S concentration and deposition time, which differ between these studies. A slight increase of the oxide reduction and H_{ads} charge in the cathodic sweep indicates the partial recovery of the Pt surface, due to

the oxidation of the S_{ads}. However, as in the case of Pt(100), the small charge of H_{des} in the first cycle suggests that reaction products adsorb and block the surface. The second cycle, however, results in a significant recovery of free Pt adsorption sites, as reflected by the increase of the H_{ads}/H_{des} charge.

Interestingly, in contrast to the results observed on Pt(100), the Pt free sites are fully recovered on the Pt(111) and Pt(221) surfaces after 4 cycles (Supporting Information, Figure S5). It is important to highlight that the electrochemical surface area (ECSA) of the Pt(111) after 4 oxidation cycles changes, due to an increase in the quantity of surface defects [52].

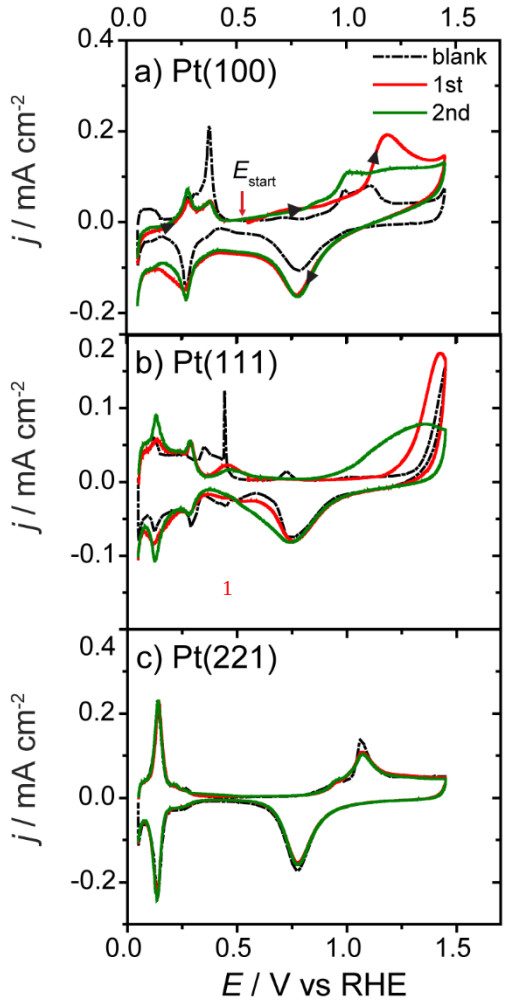

Figure 7. Voltammetric profiles of surface modified Pt(100), Pt(111), and Pt(221) electrodes in 0.5 M H_2SO_4. The dash-dotted line corresponds to the unmodified Pt single-crystal electrodes. The

red and green lines correspond to the first and second scan of a Na_2SO_3 modified electrode. Arrows in Fig. 7a indicate the start potential and scan directions. Scan rate, υ = 50 mV s^{-1}.

Studies were also extended to the regeneration of the Pt single-crystal electrodes modified in a Na_2SO_3 solution. Results are presented in Fig. 7. Blank voltammograms of unmodified electrodes are included for sake of comparison.

The first important observation appears on the CV for the Pt(221) surface. The voltammetric profiles of Pt(221) immersed in 0.1 M Na_2SO_3 solution and cycled starting from 0.5 V do not show any features associated to the oxidation of SO_3^{2-} species. On the contrary, the CVs are identical to the blank one. This indicates that the adsorption of SO_3^{2-} does not take place at open circuit potential on this surface. This further supports the idea that a specific atomic ensemble may be required for SO_3^{2-} adsorption.

On the first anodic sweep of the Pt(100) surface, a pre-wave between 0.5 and 1.1 V and a broad peak at ~1.20 V are observed. The voltammetric profiles of the Pt(100) surface after Na_2SO_3 modification also reveal an increase of the apparent double-layer and reduction currents in the low potential region ($\leq$ 0.5 V). Combined with the surface structure change due to the high potential limit (1.45 V), it is difficult to be conclusive on the full oxidation of the SO_3^{2-} species and the full recovery of the free Pt sites. However, it is reasonable to suggest that the increase of the double layer current and the reduction currents are associated to the adsorption/reduction of the reaction products due to the oxidation of SO_3^{2-} species.

The oxidation of the adsorbed species on the Pt (111) surface during the first voltammetric cycle takes place at E > 1.2 V with a maximum current density at 1.45 V. This oxidation potential is significantly higher than that observed on Pt(100). As evidenced by the presence of H_{ads} features on defects sites in the cathodic scan (peaks at 0.12 and 0.29 V in Fig. 7b and in Figure S4), the oxidation of the adsorbed sulfur species at high potentials was also

accompanied by the formation of surfaces oxides that disturbed the long-range order of the electrode. The second cycle features a new oxidation peak in the anodic sweep at potentials > 0.9 V vs RHE and an increase of the H_{ads} charge in the cathodic scan. Furthermore, the oxidation of the adsorbed sulfur species was complete after two potential cycles.

Electrochemical characterization of sulfur-modified Pt nanoparticles supported on carbon (PtNP/C)

The electrochemical behavior of sulfur species was also elucidated on PtNPs supported on Vulcan carbon (20 wt % Pt), as an example of a practical carbon-supported Pt catalyst. The voltammetric profiles of PtNP/C electrodes before and after sulfur modification with five different sulfur containing species: (a) Na_2S, (b) $Na_2S_2O_4$, (c) $Na_2S_2O_5$, (d) Na_2SO_3 and (e) SO_2 are shown in Fig. 8. The CVs were similar to those for polycrystalline platinum foil electrodes (Fig. 1), where the H_{ads}/H_{des} is suppressed due to the adsorption of the sulfur species. Hydrogen charge, Q_H, for each PtNP/C electrodes was calculated in a similar way as in Table 1 and the results are summarized in Table 3.

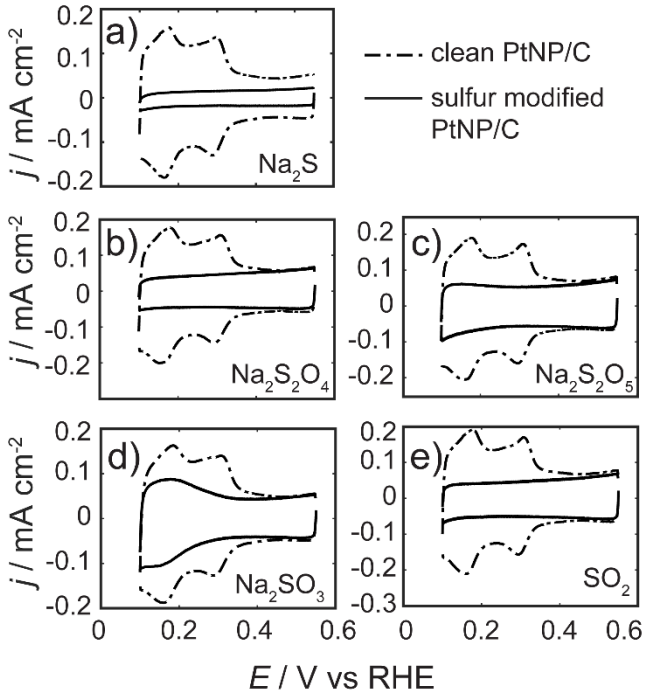

Figure 8. Voltammetric profiles of the H_{UPD} region of PtNP/C electrodes obtained before (dash-dotted line) and after (solid line) immersing in 0.1 M (a) Na_2S, (b) $Na_2S_2O_4$, (c) $Na_2S_2O_5$ (d) Na_2SO_3, (e) SO_2 solutions. All CVs were recorded in 50 mM H_2SO_4. Scan rate υ = 100 mV s^{-1}. The current values were normalized to the ECSA of each electrode, determined based on the H_{UPD} charge (see experimental section).

Table 3. Values of the hydrogen charge for the sulfur-modified PtNP/C electrodes (Q_H^S) and sulfur species coverage (θ_S) determined from the CVs in Fig. 8.

	Na_2S	$Na_2S_2O_4$	$Na_2S_2O_5$	Na_2SO_3	SO_2
Q_H^S ($\mu C\ cm^{-2}$)	0.0	0.0	5.3	53.7	0.0
θ_S	~100 %	~100 %	97 %	74 %	~100 %

Upon potential cycling up to 1.25 V vs RHE, the oxidation of the sulfur species on the PtNP/C electrodes takes place and the features associated to the H_{ads}/H_{des} are recovered over time. It is important to highlight that a full recovery of the H_{ads}/H_{des} features was not achieved until up to 50 oxidation/reduction cycles, suggesting a slower electrochemical process in comparison with the Pt polycrystalline foil electrodes. This is possibly caused by the carbon support, which may act as a reservoir for the sulfur-species or other impurities that are not easily cleaned by voltammetric cycling. The electrochemical regeneration of the poisoned PtNP/C electrodes follows a similar trend to that observed in Fig. 2. For Na_2S, the PtNP/C electrode was only partially recovered after 50 cycles.

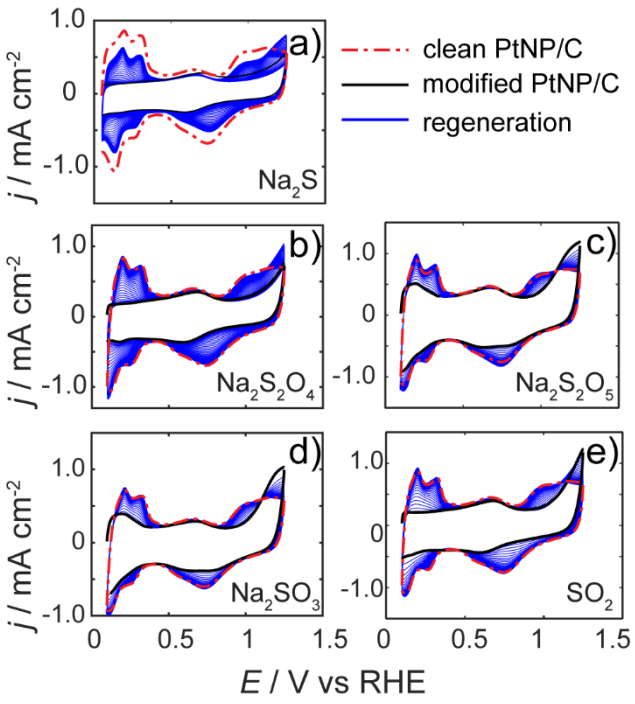

Figure 9. Voltammetric profiles of PtNP/C electrodes for modification with (a) Na_2S, (b) $Na_2S_2O_4$, (c) $Na_2S_2O_5$ (d) Na_2SO_3 and (e) SO_2. The red dash-dotted line represents the unmodified PtNP/C electrode. The solid black and green lines illustrate the voltammetric profiles recorded immediately after modification and during regeneration processes. All CVs were recorded in 50 mM H_2SO_4. All figures contain 50 consecutive cycles. Scan rate υ = 500 mV s^{-1}.

Quantitative analysis of the oxidation process of the adsorbed species on the PtNP/C is shown on Fig. 10, in terms of H_{ads}/H_{des} charge as a function of cycle number. It can be seen that upon surface modification, the H_{ads}/H_{des} features of the PtNP/C electrodes have been strongly supressed in all cases. In addition, similar to the regeneration curves obtained for the Pt foil, the PtNP/C electrode modified by Na_2S shows an initial slow recovery, then followed by the more a rapid recovery of the free active sites. In the case of $Na_2S_2O_5$, Na_2SO_3 and SO_2 modification, the hydrogen charge reached full recovery after only 20 cycles (see Fig. 10), while the PtNP/C modified with $Na_2S_2O_4$ and Na_2S required 30 and 40 cycles, respectively, to reach a plateau. Noticeably, for all electrodes, the final charge densities after 50 cycles are

lower than that for a clean Pt surface (210 μC cm^{-2}). This partial recovery might be attributed to other impurities for the Vulcan carbon support, which are difficult to remove by cycling up to 1.25 V.

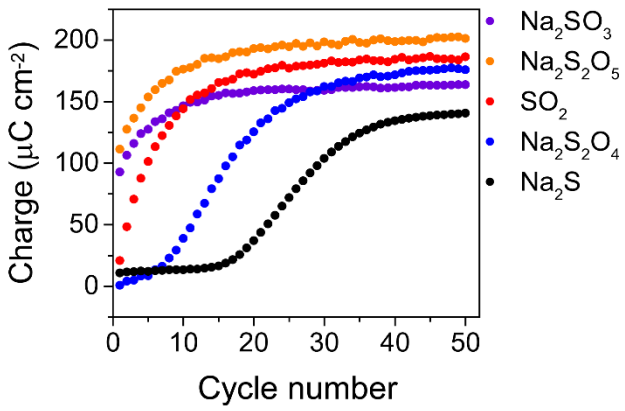

Figure 10. Relation between the hydrogen charge (normalized to ECSA) in each cathodic scan, Q_H^S, and the corresponding cycle number for PtNP/C electrodes. The charge values were obtained by integrating the cathodic traces from Fig. 9 in the potential region of 0.05 – 0.45 V.

CONCLUSIONS

In this work, we have studied the electro-oxidation of sulfur-containing species adsorbed at various types of Pt electrodes, namely polycrystalline Pt foil, Pt single-crystals and Pt nanoparticles supported on Vulcan carbon (PtNP/C). A number of sulfur compounds with different oxidation states were considered: Na_2S, $Na_2S_2O_4$, $Na_2S_2O_5$, Na_2SO_3 and SO_2. We have shown that all the Pt electrodes are sensitive to sulfur poisoning. The results on the polycrystalline Pt electrode suggest that the degree of poisoning and the rate at which the electrode is recovered upon electrochemical oxidation is associated to the oxidation state of sulfur, with 2+ being the strongest poison (most difficult to recover), 3+ less strong, and 4+ the weakest (easiest to recover). In addition, on Pt nanoparticles, the initial surface coverage was higher than on the Pt polycrystalline electrodes. The larger coverage of the sulfur species on

the Pt nanoparticles can be associated to other factors such as high density of low coordinated atoms and defects in comparison with extended polycrystalline surfaces [53]. For these two types of electrodes, the poisoned Pt surface can be regenerated by consecutive potential cycling, with an upper potential limit of 1.25 V vs RHE. The recovery rate of the Pt free sites is strongly related to the nature of the adsorbed species. We have compared electrochemical and XPS data to elucidate the chemical state of sulfur species during the recovery process and found the final reaction product is sulfate.

The studies on Pt single-crystal electrodes revealed a strong surface-structure dependence on both poison and regeneration process. For surfaces modified by S^{2-}, the most active surface towards S_{ads} oxidation was Pt(100), while both (111) and (221) showed similar oxidation behavior. In the case of Na_2SO_3 modification, the stepped surface (221) showed minimal adsorption while Pt(111) and Pt(100) showed a strong poisoning effect, suggesting that the adsorption of SO_3^{2-} requires some minimum terrace length. Importantly, the findings in this study may guide the development of catalysts which are less prone to poisoning and the advance of novel methods for catalyst regeneration.

ACKNOWLEDGEMENT

C.-H. C. thanks the U.K. Catalysis Hub for financial support. The UK Catalysis Hub is kindly thanked for resources and support provided via our membership of the consortium, funded by EPSRC (grants EP/K014706/2, EP/K014668/1, EP/K014854/1, EP/K014714/1 and EP/M013219/1). P.R.U. thanks the Royal Society for a Wolfson Research Merit Award.

ASSOCIATED CONTENT

Supporting Information

S1. Optical images of Pt nanoparticle modified glassy carbon electrode

S2. Full XPS spectra for polycrystalline electrodes modified by Na_2S

S3. Full XPS spectra for polycrystalline electrodes modified by Na_2SO_3

S4. Summary of total elemental composition from XPS spectra

S5. Summary of bond energies of S $2p_{3/2}$ peaks and the corresponding FWHM

S6. Voltammetric characterization of Pt single-crystal surfaces without modification

S7. Voltammetric characterization of single-crystal Pt electrodes modified by Na_2S

Corresponding Authors

Patrick R. Unwin, P.R.Unwin@warwick.ac.uk

Paramaconi Rodriguez, P.B.Rodriguez@bham.ac.uk

Author Contributions

Experiments on polycrystalline and nanoparticles were performed by C.-H. C. Experiments on single-crystal electrodes were performed by AH and PR. The XPS analysis was performed by C.-H. C and M. W. All authors contributed in the analysis of the results, discussion, writing and revision of the manuscript.

REFERENCES

[1] C.H. Bartholomew, Mechanisms of catalyst deactivation, Appl. Catal., A 212 (2001) 17-60.

[2] C.H. Bartholomew, P.K. Agrawal, J.R. Katzer, Sulfur Poisoning of Metals, Adv. Catal. 31 (1982) 135-242.

[3] P. Rylander, Catalytic hydrogenation over platinum metals, Elsevier, New York, 2012.

[4] J. Barbier, E. Lamy-Pitara, P. Marecot, J.P. Boitiaux, J. Cosyns, F. Verna, Role of Sulfur in Catalytic Hydrogenation Reactions, Adv. Catal. 37 (1990) 279-318.

[5] E. Protopopoff, P. Marcus, Effect of chemisorbed sulfur on the electrochemical hydrogen adsorption and recombination reactions on Pt (111), J. Vac. Sci. Technol., A 5 (1987) 944-947.

[6] F. Zaera, The Surface Chemistry of Metal-Based Hydrogenation Catalysis, ACS Catal. 7 (2017) 4947-4967.

[7] E.B. Maxted, The Poisoning of Metallic Catalysts, in: W.G. Frankenburg, V.I. Komarewsky, E.K. Rideal, P.H. Emmett, H.S. Taylor (Eds.), Adv. Catal., Academic Press1951, pp. 129-178.

[8] J.A. Rodriguez, M. Kuhn, J. Hrbek, The bonding of sulfur to a Pt(111) surface: photoemission and molecular orbital studies, Chem. Phys. Lett. 251 (1996) 13-19.

[9] J.A. Rodriguez, J. Hrbek, M. Kuhn, T. Jirsak, S. Chaturvedi, A. Maiti, Interaction of sulfur with Pt(111) and Sn/Pt(111): Effects of coverage and metal–metal bonding on reactivity toward sulfur, J. Chem. Phys. 113 (2000) 11284-11292.

[10] J.A. Rodriguez, J. Hrbek, Interaction of Sulfur with Well-Defined Metal and Oxide Surfaces: Unraveling the Mysteries behind Catalyst Poisoning and Desulfurization, Acc. Chem. Res. 32 (1999) 719-728.

[11] A. Kolics, A. Wieckowski, Adsorption of Bisulfate and Sulfate Anions on a Pt(111) Electrode, J. Phys. Chem. B 105 (2001) 2588-2595.

[12] K.E. Swider, D.R. Rolison, The Chemical State of Sulfur in Carbon‐Supported Fuel‐Cell Electrodes, J. Electrochem. Soc. 143 (1996) 813-819.

[13] K.E. Swider, D.R. Rolison, Catalytic Desulfurization of Carbon Black on a Platinum Oxide Electrode, Langmuir 15 (1999) 3302-3306.

[14] R. Mohtadi, W.k. Lee, J.W. Van Zee, Assessing durability of cathodes exposed to common air impurities, J. Power Sources 138 (2004) 216-225.

[15] T. Loučka, Adsorption and oxidation of sulphur and of sulphur dioxide at the platinum electrode, J. Electroanal. Chem. Interfacial Electrochem. 31 (1971) 319-332.

[16] T. Loučka, Adsorption and oxidation of organic compounds on a platinum electrode partly covered by adsorbed sulphur, J. Electroanal. Chem. Interfacial Electrochem. 36 (1972) 355-367.

[17] A. Zolfaghari, G. Jerkiewicz, W. Chrzanowski, A. Wieckowski, Energetics of the Underpotential Deposition of Hydrogen on Platinum Electrodes: II. Presence of Coadsorbed Sulfur, J. Electrochem. Soc. 146 (1999) 4158-4165.

[18] R.V. Bucur, State of the pre-adsorbed sulfur on a rough platinum electrode in voltammetric conditions: Microgravimetric measurements with electrochemical quartz crystal microbalance, Electrochim. Acta 87 (2013) 186-193.

[19] M.I. Awad, M.M. Saleh, T. Ohsaka, Electroactivity regeneration of sulfur-poisoned platinum nanoparticle-modified glassy carbon electrode at low anodic potentials, J. Solid State Electrochem. 19 (2015) 1331-1340.

[20] J.J. Pietron, Dual-Pathway Kinetics Assessment of Sulfur Poisoning of the Hydrogen Oxidation Reaction at High Surface-Area Platinum/Vulcan Carbon Electrodes, J. Electrochem. Soc. 156 (2009) B1322-B1328.

[21] B. Xu, I.-S. Park, Y. Li, D.-J. Chen, Y.J. Tong, An in situ SERS investigation of the chemical states of sulfur species adsorbed onto Pt from different sulfur sources, J. Electroanal. Chem. 662 (2011) 52-56.

[22] I.-S. Park, B. Xu, D.O. Atienza, A.M. Hofstead-Duffy, T.C. Allison, Y.J. Tong, Chemical State of Adsorbed Sulfur on Pt Nanoparticles, ChemPhysChem 12 (2011) 747-752.

[23] V.A. Sethuraman, J.W. Weidner, Analysis of sulfur poisoning on a PEM fuel cell electrode, Electrochim. Acta 55 (2010) 5683-5694.
[24] A.J. Appleby, B. Pichon, The mechanism of the electrochemical oxidation of sulfur dioxide in sulfuric acid solutions, J. Electroanal. Chem. Interfacial Electrochem. 95 (1979) 59-71.
[25] M.J. Foral, S.H. Langer, Characterization of sulfur layers from reduced sulfur dioxide on porous platinum black/teflon electrodes, J. Electroanal. Chem. Interfacial Electrochem. 246 (1988) 193-205.
[26] J.A. O'Brien, J.T. Hinkley, S.W. Donne, S.E. Lindquist, The electrochemical oxidation of aqueous sulfur dioxide: A critical review of work with respect to the hybrid sulfur cycle, Electrochim. Acta 55 (2010) 573-591.
[27] B.K. Kakati, A.R.J. Kucernak, K.F. Fahy, Using corrosion-like processes to remove poisons from electrocatalysts: a viable strategy to chemically regenerate irreversibly poisoned polymer electrolyte fuel cells, Electrochim. Acta 222 (2016) 888-897.
[28] Y.E. Sung, W. Chrzanowski, A. Zolfaghari, G. Jerkiewicz, A. Wieckowski, Structure of Chemisorbed Sulfur on a Pt(111) Electrode, J. Am. Chem. Soc. 119 (1997) 194-200.
[29] S.-G. Sun, S.-P. Chen, N.-H. Li, G.-Q. Lu, B.-Z. Chen, F.-C. Xu, Chemical states of bismuth and sulfur adatoms on the polycrystalline Pt electrode surface towards HCOOH oxidation — combined studies of cyclic voltammetry, in situ FTIRS and XPS on the origin of electrocatalytic activity of adatoms, Colloids Surf., A 134 (1998) 207-220.
[30] D.E. Ramaker, D. Gatewood, A. Korovina, Y. Garsany, K.E. Swider-Lyons, Resolving Sulfur Oxidation and Removal from Pt and Pt3Co Electrocatalysts Using in Situ X-ray Absorption Spectroscopy, J. Phys. Chem. C 114 (2010) 11886-11897.
[31] M.E. Gamboa-Aldeco, E. Herrero, P.S. Zelenay, A. Wieckowski, Adsorption of bisulfate anion on a Pt(100) electrode: A comparison with Pt(111) and Pt(poly), J. Electroanal. Chem. 348 (1993) 451-457.
[32] Y.E. Sung, W. Chrzanowski, A. Wieckowski, A. Zolfaghari, S. Blais, G. Jerkiewicz, Coverage evolution of sulfur on Pt(111) electrodes: From compressed overlayers to well-defined islands, Electrochim. Acta 44 (1998) 1019-1030.
[33] O.A. Baturina, K.E. Swider-Lyons, Effect of SO2 on the Performance of the Cathode of a PEM Fuel Cell at 0.5–0.7 V, J. Electrochem. Soc. 156 (2009) B1423-B1430.
[34] J. Fu, M. Hou, C. Du, Z. Shao, B. Yi, Potential dependence of sulfur dioxide poisoning and oxidation at the cathode of proton exchange membrane fuel cells, J. Power Sources 187 (2009) 32-38.

[35] C. Quijada, E. Morallón, J.L. Vázquez, L.E.A. Berlouis, Electrochemical behaviour of aqueous SO2 at polycrystalline gold electrodes in acidic media. A voltammetric and in-situ vibrational study. Part II. Oxidation of SO2 on bare and sulphur-modified electrodes, Electrochim. Acta 46 (2001) 651-659.
[36] C. Quijada, A. Rodes, F. Huerta, J.L. Vázquez, In situ FT–IRRAS study of SO2 adlayers formed on Pt(111) electrodes from open-circuit adsorption in acidic media, Electrochim. Acta 44 (1998) 1091-1096.
[37] C. Quijada, A. Rodes, J.L. Vázquez, J.M. Pérez, A. Aldaz, Electrochemical behaviour of aqueous sulphur dioxide at polycrystalline Pt electrodes in acidic medium. A voltammetric and in-situ FT-IR study Part II. Promoted oxidation of sulphur dioxide. Reduction of sulphur dioxide, J. Electroanal. Chem. 398 (1995) 105-115.
[38] E. Herrero, V. Climent, J.M. Feliu, On the different adsorption behavior of bismuth, sulfur, selenium and tellurium on a Pt(775) stepped surface, Electrochem. Commun. 2 (2000) 636-640.
[39] P. Marcus, E. Protopopoff, Coadsorption of sulphur and hydrogen on platinum (110) studied by radiotracer and electrochemical techniques, Surf. Sci. 161 (1985) 533-552.
[40] S. Trasatti, O.A. Petrii, Real surface area measurements in electrochemistry, J. Electroanal. Chem. 327 (1992) 353-376.
[41] Y. Garsany, I.L. Singer, K.E. Swider-Lyons, Impact of film drying procedures on RDE characterization of Pt/VC electrocatalysts, J. Electroanal. Chem. 662 (2011) 396-406.
[42] J. Monzo, D.F. van der Vliet, A. Yanson, P. Rodriguez, Elucidating the degradation mechanism of the cathode catalyst of PEFCs by a combination of electrochemical methods and X-ray fluorescence spectroscopy, Phys. Chem. Chem. Phys. 18 (2016) 22407-22415.
[43] M.J. Vasile, C.G. Enke, The preparation and thermodynamic properties of a palladium-hydrogen electrode, J. Electrochem. Soc. 112 (1965) 865-70.
[44] V. Climent, J.M. Feliu, Thirty years of platinum single crystal electrochemistry, J. Solid State Electrochem. 15 (2011) 1297-1315.
[45] J. Solla-Gullon, P. Rodriguez, E. Herrero, A. Aldaz, J.M. Feliu, Surface characterization of platinum electrodes, Phys. Chem. Chem. Phys. 10 (2008) 1359-1373.
[46] A. Cuesta, Atomic Ensemble Effects in Electrocatalysis: The Site-Knockout Strategy, ChemPhysChem 12 (2011) 2375-2385.
[47] B.J. Lindberg, K. Hamrin, G. Johansson, U. Gelius, A. Fahlman, C. Nordling, K. Siegbahn, Molecular Spectroscopy by Means of ESCA II. Sulfur compounds. Correlation of electron binding energy with structure, Phys. Scr. 1 (1970) 286.

[48] C.-J. Zhong, N.T. Woods, G.B. Dawson, M.D. Porter, Formation of thiol-based monolayers on gold: implications from open circuit potential measurements, Electrochem. Commun. 1 (1999) 17-21.
[49] J. Clavilier, R. Faure, G. Guinet, R. Durand, Preparation of monocrystalline Pt microelectrodes and electrochemical study of the plane surfaces cut in the direction of the {111} and {110} planes, J. Electroanal. Chem. 107 (1980) 205-209.
[50] J. Clavilier, R. Durand, G. Guinet, R. Faure, Electrochemical adsorption behaviour of Pt(100) in sulphuric acid solution, J. Electroanal. Chem. Interfacial Electrochem. 127 (1981) 281-287.
[51] A.M. Gómez-Marín, R. Rizo, J.M. Feliu, Some reflections on the understanding of the oxygen reduction reaction at Pt(111), Beilstein J. Nanotechnol. 4 (2013) 956-967.
[52] A. Björling, J.M. Feliu, Electrochemical surface reordering of Pt(111): A quantification of the place-exchange process, J. Electroanal. Chem. 662 (2011) 17-24.
[53] C. Vericat, G.A. Benitez, D.E. Grumelli, M.E. Vela, R.C. Salvarezza, Thiol-capped gold: from planar to irregular surfaces, J. Phys.: Condens. Matter 20 (2008) 184004.